Coherent double-pulse control of quantum beats in a coupled quantum well

Marie S. C. Luo and Shun Lien Chuang
Department of Electrical and Computer Engineering, University of Illinois at Urbana-Champaign, 1406 West Green Street, Urbana, Illinois 61801-2991

Paul C. M. Planken, Igal Brener, and Martin C. Nuss
AT&T Bell Laboratories, 101 Crawfords Corner Road, Holmdel, New Jersey 07733-3030
(Received 22 March 1993)

Analytical and numerical solutions for coherent excitations of quantum beats in a coupled quantum well by two phase-locked optical pulses are shown using the density-matrix formulation. It is demonstrated that active control of terahertz radiation due to charge oscillations caused by quantum beats in a coupled-quantum-well structure is possible using two-femtosecond optical pulses with a time delay shorter than the exciton dephasing time. Our theoretical results agree very well with experimental observations.

I. INTRODUCTION

Recently, charge oscillations in a coupled-quantum-well structure have been observed[1] directly from the terahertz generation emitted by the oscillations after coherent excitation by a femtosecond optical pulse. The pulse duration is typically on the order of 100 fs, and by biasing the quantum wells near the resonant field such that two electron states in the narrow well and the wide well are aligned, multiple oscillations appear in the generated terahertz signals. Previously, quantum beats have been observed in a degenerate four-wave-mixing experiment.[2] Terahertz radiation has also been generated from the surface[3] of semiconductors using femtosecond pulses as long as the optical pump energy is above the band gap of the materials. An optical rectification theory has been proposed[4] to explain all of the observed major phenomena, including the crystal orientation dependence of the terahertz radiation intensity, which cannot be explained using the photoconduction current model[3] since the photoconductivity of a zinc-blende structure is isotropic.

From the nonlinear optics point of view, the terahertz generation from bulk materials and quantum wells can be explained from the second-order nonlinear susceptibility for difference-frequency generation, $\chi^{(2)}(\omega_1-\omega_2;\ \omega_1,\omega_2)$. Within a three-level model,[1] we find that the induced terahertz radiation field in the presence of the optical pump consists of two major contributions: one from the diagonal terms of the density matrix or the induced "populations" of each level, which follows the optical pumping signal adiabatically; the other from the off-diagonal terms of the density matrix, corresponding to the quantum beats of two nearby levels. In the case of terahertz generation from the surface of bulk semiconductors, the instantaneous optical rectification current[4] is dominant since quantum beats among continuum states in the depletion region of a semiconductor do not show up and a ballistic transport current may also appear. The optical rectification effect can clearly be demonstrated[5] using a quantum-well structure pumped with a photon energy between the band gaps of the quantum wells and the barriers. In this way, current transport is inhibited in the direction perpendicular to the wells. Bulk optical rectification effects have also been observed[6] using a normal incidence geometry in which any induced current normal to the semiconductor surface, if there is any, cannot radiate in the normal direction. Terahertz generation due to both optical rectification and quantum beats of the light-hole and heavy-hole excitons has also been demonstrated[7] and explained using the difference-frequency generation, or optical rectification theory for a three-level model.

Ideally, precise control over both the duration and the shape of the generated terahertz transients is desired. Different schemes have to be studied to shape the terahertz electromagnetic wave form. One method is to excite the material with a pulse sequence, more specifically, a coherent multipulse sequence. The work on the generation of coherent light pulses with controlled amplitude and phase began in the 1970s, with interest stemming from its applications in communications, signal processing, and time-resolved spectroscopy. The first attempt was to shape the optical pulse by spatial filtering with diffraction gratings, but the resulting pulses were chirped.[8] Picosecond pulse shaping was reported in the 1980s with different approaches ranging from spectral masking to grating pulse compression. Shaping control[9] has been accomplished at all optical wavelengths and for a pulse separation less than 25 ps. Pulse shaping[10] has been achieved by passing a single femtosecond pulse through a transient grating and specially designed phase masks. Different wave forms can be synthesized and terahertz-rate trains of pulses have been created.

Most recently, coherent control of quantum beats or optical rectification has been demonstrated[11] for the first time in an asymmetric coupled-quantum-well structure using two phase-locked optical pulses. A schematic description of the experiment is shown in Fig. 1(a). The sample consists of ten pairs of wide-well (WW) and narrow-well (NW) regions which are separated by a 25-

0163-1829/93/48(15)/11043(8)/$06.00

Å-thick $Al_{0.2}Ga_{0.8}As$ barrier. Both wells are made of a GaAs layer with 145 Å for the WW and 100 Å for the NW. The pairs are isolated from each other by 200-Å-wide buffer layers and capped with 3500-Å-thick $Al_{0.2}Ga_{0.8}As$ layers. All regions are undoped except the n-type GaAs substrate. It is shown that by tuning the pump energy near the resonance of the two coupled exciton states of the two electron subbands and the heavy-hole subband in the narrow well, the generated terahertz radiation can be either enhanced, weakened, or phase shifted by controlling the relative time delay and phase difference between the two optical pulses. These experiments using phase-locked optical pulses in semiconductors to control quantum beats[11] were only possible because of the availability of stable femtosecond laser pulses around 800 nm and the relatively long dephasing times of excitons (a few picoseconds) in high-quality quantum wells at low temperatures. These have also been the first experiments to temporally resolve the phase shifts associated with these coherent double-pulse phenomena.

In this paper, we present a detailed theory for the coherent control of the terahertz generation due to quantum beats in the coupled-quantum-well structure using two phase-locked optical pulses. The delayed pulse can either reinforce or weaken the oscillations, depending on the phase difference and the delay time between the two pulses. This is quite surprising at first glance because one would expect that the generation of charge oscillations by optical rectification only depends on the intensities $|E|^2$ of the optical pulses and hence should be insensitive to their relative phase differences. As we will show later, the relative phase between the laser pulses plays an important role. Analytical results are obtained in Sec. II by assuming that the exciting optical pulses are δ functions. These analytical solutions show the most significant features of physics and will be discussed in detail. From these results we can understand how one can enhance, weaken, or phase-shift terahertz radiation by tuning the phase difference and the time delay between the optical pulses. The simulated results that take into account the finite pulse durations by solving the nonlinear density-matrix equations numerically will then be presented in Sec. III with comparisons to experimental observations. The multiple-pulse sequence excitation will be investigated in Sec. IV, followed by the conclusions.

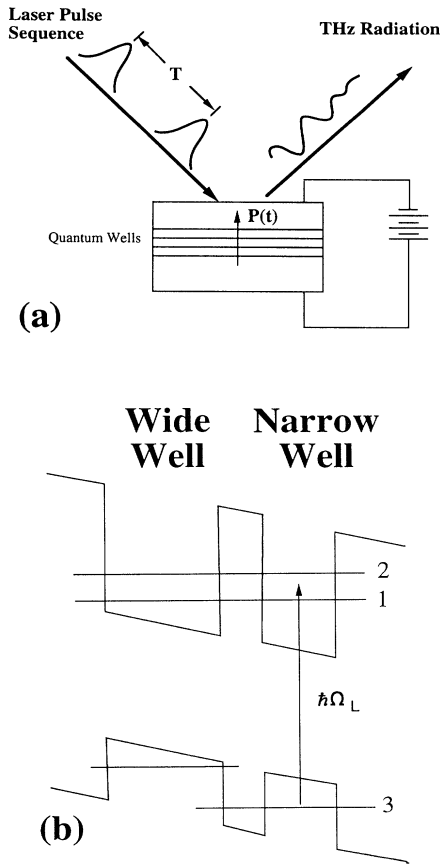

FIG. 1. (a) The schematic diagram of two-pulse excitation. (b) Energy-band diagram for a three-level model in an asymmetric coupled-quantum-well system.

II. ANALYTICAL SOLUTIONS OF TWO-δ-PULSE EXCITATIONS

In this section, we consider a three-level model in an asymmetric coupled-quantum-well structure as described[1] in Sec. I. The two coupled conduction subbands between the narrow well and the wide well are denoted as level 1 and level 2, and the heavy-hole subband in the narrow well is designated as level 3, as shown in Fig. 1(b). Because the duration of the laser pulse is about a hundred femtoseconds and its amplitude is smooth within an optical cycle, the laser field amplitude is assumed to be

$$E(t)=E_L(t)e^{-i\Omega_L t}+E_L^*(t)e^{i\Omega_L t}, \tag{1}$$

where the envelope function $E_L(t)$ is slowly varying compared with the optical frequency Ω_L. The optical energy is close to the band edge of the semiconductor quantum wells. When calculating the density-matrix elements, we can therefore make the rotating wave approximation, which neglects all but near-resonance terms. Let

$$\begin{aligned}&\rho_{11}=\rho_{11}(t)\ ,\quad \rho_{22}=\rho_{22}(t)\ ,\quad \rho_{33}=\rho_{33}(t)\ ,\\ &\rho_{12}=\rho_{12}(t)\ ,\\ &\rho_{13}=\rho_{13}(t)e^{-i\Omega_L t}\ ,\quad \rho_{23}=\rho_{23}(t)e^{-i\Omega_L t}\ ,\end{aligned} \tag{2}$$

where $\rho_{nm}=\langle n|\rho|m\rangle$ is the matrix element of the original density operator; ρ_{nm} describes the mixing between energy states n and m, and is equal to the population of the level is $n=m$. The equations of motion[12] for the density-matrix elements can be written explicitly as follows:

$$\begin{aligned}\frac{\partial\rho_{11}(t)}{\partial t}=&-\frac{\rho_{11}(t)-\rho_{11}^{(0)}}{T_{11}}\\ &+\frac{i}{\hbar}[\mu_{13}\rho_{31}(t)E_L(t)-\rho_{13}(t)\mu_{31}E_L^*(t)]\ ,\end{aligned} \tag{3}$$

$$\frac{\partial\rho_{33}(t)}{\partial t}=-\frac{\rho_{33}(t)-\rho_{33}^{(0)}}{T_{33}}-\frac{i}{\hbar}\{[\rho_{31}(t)\mu_{13}+\rho_{32}(t)\mu_{23}]E_L(t)-[\mu_{31}\rho_{13}(t)+\mu_{32}\rho_{23}(t)]E_L^*(t)\}\ , \tag{4}$$

$$\frac{\partial\rho_{12}(t)}{\partial t}=-\left[i\omega_{12}+\frac{1}{T_{12}}\right]\rho_{12}(t)+\frac{i}{\hbar}[\mu_{13}\rho_{32}(t)E_L(t)-\rho_{13}(t)\mu_{32}E_L^*(t)]\ , \tag{5}$$

$$\frac{\partial\rho_{13}(t)}{\partial t}=-\left[i\Delta_{13}+\frac{1}{T_{13}}\right]\rho_{13}(t)+\frac{i}{\hbar}\{\mu_{13}[\rho_{33}(t)-\rho_{11}(t)]E_L(t)-\rho_{12}(t)\mu_{23}E_L(t)\}\ , \tag{6}$$

with a similar equation to (3) for $\rho_{22}(t)$ and another equation similar to (6) for $\rho_{23}(t)$ except that we exchange the subscript 1 with 2. Here μ_{nm} are the dipole moments between states n and m, $\hbar\Delta_{13}=\varepsilon_{13}-\hbar\Omega_L$ and $\hbar\Delta_{23}=\varepsilon_{23}-\hbar\Omega_L$ are the detuning energies, and $\hbar\omega_{21}=-\hbar\omega_{12}=\varepsilon_{23}-\varepsilon_{13}$ is the intersubband energy splitting.

The simplest pulse sequence consists of two pulses and will be studied first. We assume that each pulse duration is so short compared with the system response times (the dephasing time and the period of quantum beat in this case) that the optical fields can be described by impulsive functions. This assumption leads to analytical results from which we gain physical insight. The numerical results taking into account finite-pulse durations will be presented in Sec. III. Let

$$E_L(t)=E_1\delta(t)+E_2\delta(t-T)\ , \tag{7}$$

where E_1 and E_2 are the laser fields for the two pulses and contain both the amplitude and phase information, and T is the time delay of the second pulse from the first one as shown in Fig. 1(a). Before laser excitation, the sample is at thermal equilibrium and only the valence-band state is occupied. Therefore the initial conditions are assumed as below:

$$\rho_{11}^{(0)}=0\ ,\quad \rho_{22}^{(0)}=0\ ,\quad \rho_{33}^{(0)}=1\ ,\quad \text{and all other } \rho_{ij}^{(0)}=0\ . \tag{8}$$

For laser intensities small compared to the saturation intensity, perturbation expansions can be used to calculate the density-matrix elements. From the optical Bloch equations, the dominant contributions come from the first-order expansion for interband matrix elements and the second-order expansion for intersubband or population matrix elements. Based on these observations, the density-matrix elements, ρ_{13} and ρ_{23}, are

$$\rho_{13}^{(1)}(t)=\frac{i}{\hbar}\int_{-\infty}^{t}dt'e^{-(i\Delta_{13}+1/T_{13})(t-t')}\mu_{13}E_L(t')=\frac{i\mu_{13}}{\hbar}[E_1e^{-(i\Delta_{13}+1/T_{13})t}\Theta(t)+E_2e^{-(i\Delta_{13}+1/T_{13})(t-T)}\Theta(t-T)] \tag{9}$$

and there is a similar expression for $\rho_{23}^{(1)}(t)$ with the subscripts 13 replaced by 23, where Θ is the unit step function. With the above first-order results, the density-matrix element $\rho_{12}(t)$ comes from the second-order perturbation and can be derived as

$$\rho_{12}^{(2)}(t)=\frac{i}{\hbar}\int_{-\infty}^{t}dt'e^{-(i\omega_{12}+1/T_{12})(t-t')}[\mu_{13}\rho_{32}^{(1)}(t')E_L(t')-\mu_{32}\rho_{13}^{(1)}(t')E_L^*(t')]$$
$$=\frac{\mu_{13}\mu_{32}}{\hbar^2}[|E_1|^2e^{-(i\omega_{12}+1/T_{12})t}\Theta(t)+|E_2|^2e^{-(i\omega_{12}+1/T_{12})(t-T)}\Theta(t-T)+E_1E_2^*e^{-(i\omega_{12}+1/T_{12})(t-T)}e^{-(i\Delta_{13}+1/T_{13})T}\Theta(t-T)$$
$$+E_1^*E_2e^{-(i\omega_{12}+1/T_{12})(t-T)}e^{(i\Delta_{23}-1/T_{23})T}\Theta(t-T)]\ . \tag{10}$$

The population matrix elements are also from the second-order perturbation. We obtain

$$\rho_{11}^{(2)}(t)=\frac{i}{\hbar}\int_{-\infty}^{t}dt'e^{-(t-t')/T_{11}}[\mu_{13}\rho_{31}^{(1)}(t')E_L(t')-\mu_{31}\rho_{13}^{(1)}(t')E_L^*(t')]$$
$$=\frac{|\mu_{13}|^2}{\hbar^2}[|E_1|^2e^{-t/T_{11}}\Theta(t)+|E_2|^2e^{-(t-T)/T_{11}}\Theta(t-T)+E_1E_2^*e^{-(t-T)/T_{11}}e^{-(i\Delta_{13}+1/T_{13})T}\Theta(t-T)$$
$$+E_1^*E_2e^{-(t-T)/T_{11}}e^{(i\Delta_{13}-1/T_{13})T}\Theta(t-T)] \tag{11}$$

and a similar expression for $\rho_{22}^{(2)}(t)$ with the subscripts 13 replaced by 23 and T_{11} by T_{22} in the final form of (11). If all the longitudinal times are equal, we have $\rho_{33}^{(2)}(t)=1-\rho_{11}^{(2)}(t)-\rho_{22}^{(2)}(t)$. The number in the superscript parentheses of each matrix element indicates the order of expansion. Here, we will consider only the charge oscillations which result mainly from the density-matrix element ρ_{12} since the other terms (the diagonal terms) contribute very little to the optically induced polarization current at this small bias field. The evolutions of level populations will be discussed in Sec. III.

In order to obtain a simple physical picture, we will first assume infinite relaxation time constants. Let $|E_1|=|E_2|=E_0$ and $E_2=E_1e^{i\phi}$; then, Eq. (10) gives

$$\rho_{12}(t)=\frac{\mu_{13}\mu_{32}}{\hbar^2}E_0^2[e^{-i\omega_{12}t}\Theta(t)+e^{-i\omega_{12}(t-T)}\Theta(t-T)+e^{-i\phi}e^{-i\omega_{12}(t-T)}e^{-i\Delta_{13}T}\Theta(t-T)+e^{i\phi}e^{-i\omega_{12}(t-T)}e^{i\Delta_{23}T}\Theta(t-T)] . \tag{12}$$

The evolution of charge oscillations clearly depends on the detuning energy, the pulse delay time, and the relative phase between the two pulses. We will look at two special cases of time delay T. Note that $\Delta_{23}T-\Delta_{13}T=\omega_{21}T=-\omega_{12}T$.

Case (I): $\omega_{21}T=2n\pi$ $(n=0,1,2,\ldots)$.

$$\mathrm{Re}[\rho_{12}(t)]=\frac{\mu_{13}\mu_{32}}{\hbar^2}|E_0|^2\cos(\omega_{12}t)[\Theta(t)+\Theta(t-T)+2\cos(\phi+\Delta_{13}T)\Theta(t-T)] . \tag{13}$$

$$\text{If } \Delta_{13}T=0 \text{ or } \pm 2\pi \text{ , then } \begin{cases}\text{constructive interference: } \phi=0\\ \text{destructive interference: } \phi=\pi ;\end{cases} \tag{14}$$

$$\text{If } \Delta_{13}T=\pm\pi \text{ , then } \begin{cases}\text{constructive interference: } \phi=\pi\\ \text{destructive interference: } \phi=0 .\end{cases} \tag{15}$$

Case (I) has the second pulse delayed by one or several oscillation periods. Suppose we consider a time delay of one period first, $\omega_{21}T=2\pi$. The laser photon energy determines if the oscillations are accelerated or impeded. For pumping at the lower conduction-band edge ($\Delta_{13}=0$), the second pulse with a zero relative phase will add a driving force and the oscillating signal is quadrupled, but a pulse with a π-phase difference would suppress the oscillations, as can be seen from Eqs. (13) and (14). The opposite situation occurs if the photon energy is tuned to the middle of the two interband transitions, i.e., $\Delta_{23}T=-\Delta_{13}T=\omega_{21}T/2=\pi$, Eq. (15). On the other hand, if we consider a time delay of *two* oscillation periods ($\omega_{21}T=4\pi$), pumping at the middle of levels 1 and 2 gives $\Delta_{23}T=-\Delta_{13}T=\omega_{21}T/2=2\pi$. Therefore we have constructive interference for $\phi=0$ and destructive interference for $\phi=\pi$, following Eq. (14).

Case (II): $\omega_{21}T=(2n+1)\pi$.

$$\mathrm{Re}[\rho_{12}(t)]=\frac{\mu_{13}\mu_{32}}{\hbar^2}|E_0|^2 \times\{[\Theta(t)-\Theta(t-T)]\cos(\omega_{12}t) +2\sin(\phi+\Delta_{13}T)\sin(\omega_{12}t)\Theta(t-T)\} . \tag{16}$$

$$\text{If } \Delta_{13}T=0 \text{ , then } \begin{cases}\text{maximum: } \phi=\pi/2\\ \text{minimum: } \phi=0 \text{ or } \pi ;\end{cases} \tag{17}$$

$$\text{If } \Delta_{23}=-\Delta_{13} \text{ , then } \begin{cases}\text{maximum: } \phi=0 \text{ or } \pi\\ \text{minimum: } \phi=\pi/2 .\end{cases} \tag{18}$$

For case (II), the second pulse has a delay time equal to half (or plus an integer multiple) of the oscillation periods and the charge-oscillation signal would be doubled or terminated, depending on the photon energy. It is evident that the phase relations of the second optical pulse with respect to the first are crucial in determining the responses of pulse-sequence excitations.

Once the density-matrix elements are found, the induced polarization density can be calculated.

$$P(t)\propto|e|\{\rho_{11}(t)(z_{33}-z_{11})+\rho_{22}(t)(z_{33}-z_{22}) -2z_{12}\mathrm{Re}[\rho_{12}(t)]\} , \tag{19}$$

where ez_{ij} are the dipole moments between levels i and j. The terahertz radiation field is then obtained from the second derivative of the induced polarization density, $E_R(t)\propto\partial^2P(t)/\partial t^{(2)}$, as can be derived from Maxwell's equations.

III. NUMERICAL RESULTS OF TWO-FINITE-PULSE EXCITATION AND COMPARISON WITH EXPERIMENT

In the preceding section, δ-function pulses were used to obtain analytical results for physical understanding. But the δ function may not necessarily be a good choice, especially if the pulse duration is comparable to the inverse Rabi frequency or the oscillation period. Here, we numerically solve the systems of the density-matrix equations by the Runge-Kutta method for two optical pulses with finite-pulse durations. We will see that most of the numerical results presented in this section are similar to those analytical solutions discussed in Sec. II. Both the infinite and finite relaxation times will be studied.

A. Infinite relaxation time

The electronic potential profiles and energy-band structures of the coupled wells at different bias conditions are the same as in the coupled-quantum-well structure in Ref. 1. When the dc electric field (due to the built-in field only in this case) is small, the major contribution to the charge oscillation comes from the heavy-hole excitons in the narrow well. The two exciton energies calculated using an exciton Green's-function[13] approach are about 1.5426 and 1.5486 eV, respectively. We will consider this bias condition and look only at the excitonic response. Two different cases will be discussed as in Sec. II.

Case (I): $\omega_{21}T=2n\pi$. According to the analytical solutions, the optical wavelength is a critical parameter. We consider two possibilities: (i) pumping at the middle of levels 1 and 2 ($\Delta_{23}=-\Delta_{13}=\omega_{21}/2$) and (ii) pumping at the band edge ($\Delta_{13}=0$).

Figure 2 shows the terahertz radiation fields for pumping at the middle of levels 1 and 2 with a pulse delay of *one* oscillation period, $T_p=2\pi/\omega_{21}$. The two individual

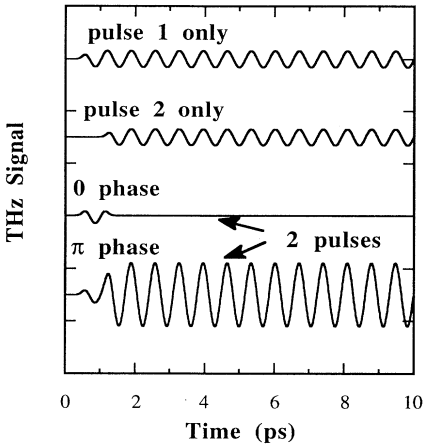

FIG. 2. The terahertz (THz) radiation signals for pumping at the *middle* of levels 1 and 2 ($\Delta_{13}=-\Delta_{23}$). The top two curves are terahertz signals due to one-pulse excitation only (optical pulse 1 and pulse 2, respectively). The bottom two curves are the responses due to both pulses 1 and 2, with zero-phase and π-phase difference, respectively. The pulse delay time T is 689 fs, which is equal to one charge-oscillation period, T_p.

pulses generate identical electromagnetic transient signals but are delayed in time. When both laser pulses illuminate the sample, the oscillating signal would be enhanced for a π-phase difference and terminated for a 0-phase difference. These results are exactly as expected from Eq. (15). Note that the magnitude of the signal for the π-phase case is increased by a factor of 4. If the photon energy is tuned to the band edge ($\Delta_{13}=0$), the results are shown in Fig. 3 and correspond to Eq. (14). The effects result from the interference between the coherent quantum beats excited by two pulses. As long as the separation of the two pulses is an integer multiple of the quantum beat period, the results may be explained by looking at the power spectrum of the pulse pair. Consider two coherent fields, E_A and E_B, and the interference of the two fields gives an intensity I,

$$E=E_A+E_Be^{i\phi}$$
$$\Rightarrow I=|E|^2=|E_A|^2+|E_B|^2+2E_AE_B\cos\phi\ . \quad (20)$$

If $E_A=E_B$, the constructive interference ($\phi=0$) increases the signal by 4, while the destructive interference ($\phi=\pi$) completely cancels out. However, when the separation between the two pulses is not an integer multiple of the quantum beat period, this simple argument fails miserably. Below, we will present a simple pseudovector model that can illustrate all the observed phenomena in an intuitive way.

With a pulse delay of *two* oscillation periods, $2T_p$, and pumping at the middle, the phase condition for the constructive result changes from the π phase (see Fig. 2) to the zero phase (see Fig. 4). It is important to realize that the second pulse also influences the *population levels.* In Fig. 5(a), the populations for the first and second levels, ρ_{11} and ρ_{22}, increase by a factor of 4 with the arrival of the second zero-phase pulse at about 1.5 ps. But if the second pulse has a π-phase shift, the two electronic levels would be depopulated as shown in Fig. 5(b).

Case (II): $\omega_{21}T=(2n+1)\pi$. We consider a pulse delay of $2.5T_p$ and photon pumping at the middle. From the individual response shown in Fig. 6, there is a π-phase shift (or sign change) as evident from the crest of pulse 1 and the trough of pulse 2. There is also an increase of signal amplitude for the 0 and π phases but nearly no charge oscillation for the $\pi/2$ condition. Notice that there is a phase shift between the zero-phase and the π-phase signals. These results are as expected from Eqs. (16)–(18).

The above findings can be explained in an intuitive way using a pseudovector presentation of Eq. (12). We represent the four terms in Eq. (12) by vectors rotating with the quantum beat frequency ω_{21}, noting the common

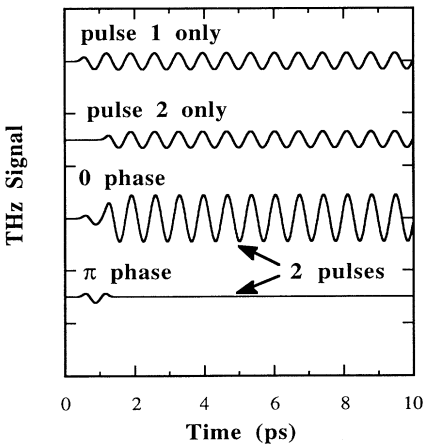

FIG. 3. Terahertz signals with laser pumping at the *lower conduction-band edge* ($\Delta_{13}=0$). The top two curves are terahertz signals due to one-pulse exception only (optical pulse 1 and pulse 2, respectively). The bottom two curves are the responses due to both pulses 1 and 2, with zero-phase and π-phase difference, respectively. The second pulse is delayed by one oscillation period, T_p.

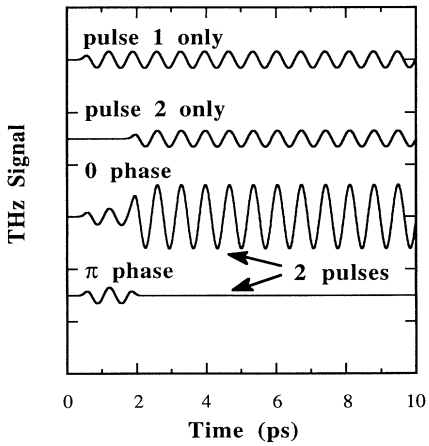

FIG. 4. The induced radiation fields with laser pumping at the *middle* of levels 1 and 2 ($\Delta_{13}=-\Delta_{23}$) and a pulse delay of *two* oscillation periods, $T=2T_p$.

$\exp(-i\omega_{21}t)$ dependence. While the first two terms correspond to the terahertz transients resulting from each of the two pulses, the last two terms are mixing terms, where one light field comes from the first pulse and the other light field from the second pulse, and vice versa. The phase relation of these four pseudovectors is hence determined by the time delay T, the energy detunings Δ_{13}, Δ_{23}, and the phase factor ϕ. We then arrive at a simple representation of how the different terms in Eq. (12) contribute to the terahertz radiation (Fig. 7). For case (I), $\omega_{21}T=2n\pi$, i.e., a pulse separation that is an integer multiple of the quantum beat period, the first two pseudovectors are always collinear. In the particular situation of $\Delta_{23}T=-\Delta_{13}T=2\pi$ (pumping at the middle of levels 1 and 2, and $n=2$), the latter two vectors are collinear with the first two for $\phi=0$, as shown in Fig. 7(a), leading to constructive interference. For $\phi=\pi$, however, the latter ones are antiparallel to the first, corresponding to destructive interference, as shown in Fig. 7(b). For case (II), $\omega_{21}T=\pi$, the first two vectors are always antiparallel, corresponding to cancellation of the first two terms in Eq. (12). Again, assuming $\Delta_{23}T=-\Delta_{13}T=\pi/2$ (pumping at the middle of levels 1 and 2), the last two vectors are in phase, but rotated by -90 ° for $\phi=0$, Fig. 7(c); or by 90 ° for $\phi=\pi$, Fig. 7(d). These correspond to

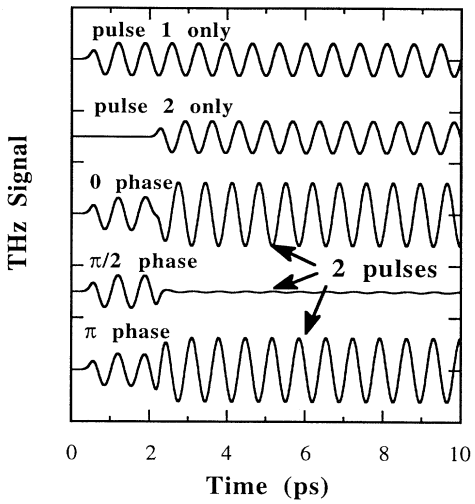

FIG. 6. Calculated terahertz signals when the second pulse is delayed by $2.5T_p$ with a phase difference of zero, $\pi/2$, and π, respectively. The other parameters are the same as those in Fig. 2.

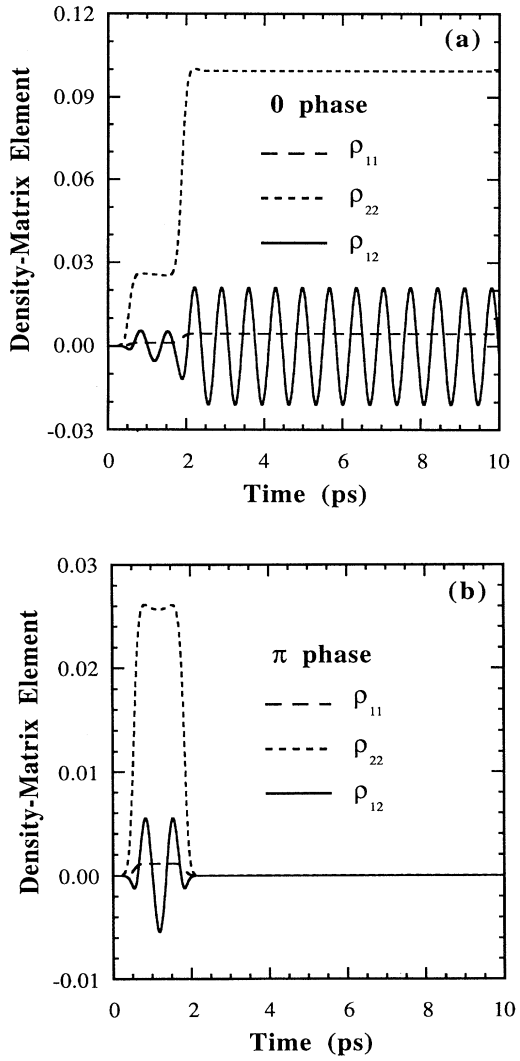

FIG. 5. (a) Time evolution of the two level populations (ρ_{11} and ρ_{22}) and the density-matrix element (ρ_{12}) when the second pulse has zero-phase difference and a delay time of $2T_p$. (b) Time evolution of the two level populations (ρ_{11} and ρ_{22}) and the density-matrix element (ρ_{12}) when the second pulse has π-phase difference and a delay time of $2T_p$.

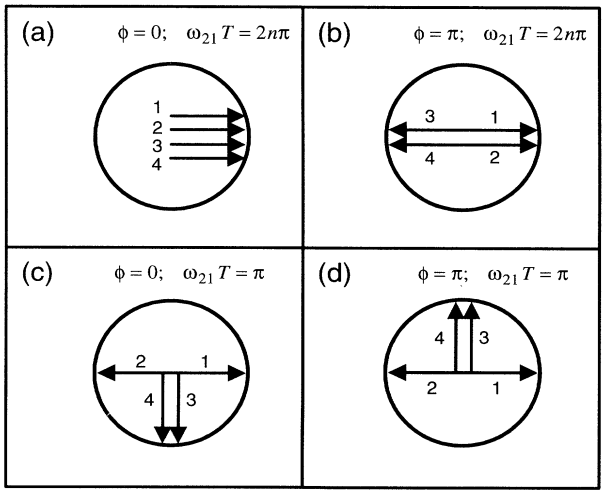

FIG. 7. Pseudovector representation of Eq. (12) for four specific cases. The numbers next to the vectors label the four terms in Eq. (12). Here we consider case (I) in the text with $\omega_{21}T=2n\pi$, $\Delta_{23}T=-\Delta_{13}T=2\pi$ (pumping at the middle of levels 1 and 2, $n=2$), and (a) $\phi=0$, (b) $\phi=\pi$. For case (II), $\omega_{21}T=\pi$, and $\Delta_{23}T=-\Delta_{13}T=\pi/2$ (pumping at the middle of levels 1 and 2), the last two vectors are in phase, but rotated by -90 ° for (c) $\phi=0$, or by 90 ° for (d) $\phi=\pi$.

the phase shifts of $\pm\pi/2$ seen in Fig. 6. For $\phi=\pi/2$ (not shown), the last two terms are antiparallel to each other, which leads to destructive interference.

B. Finite relaxation time and comparison with experiment

We have ignored all of the relaxation phenomena in Eqs. (12)–(18) to show clearly the physical meanings of the simulation data. However, excitons have a finite dephasing time,[14] typically a few picoseconds at low temperatures. As an example, we will consider case (I) discussed in Sec. III A, but with a finite relaxation time constant. In Fig. 8(a), we show the experimental data[11] for which the pump wavelength is set at the middle of level 1 and level 2 and the second pulse has a delay time of $2T_p$. The experimental setup[11] uses 80-fs, 15-nJ pulses from a mode-locked, 82-MHz repetition rate, argon-ion-pumped Ti:sapphire laser, tunable around 800 nm. The laser beam is then split in two: one beam is sent into a Michelson interferometer with its arms set at different delays to separate the emerging pulses in the time domain. One of the end mirrors of the Michelson interferometer is also mounted onto a piezoelectric transducer (PZT) to actively stabilize the length of the arm to within a fraction of the wavelength. The polarization of the light is in the plane of incidence and the laser is tuned to the narrow-well interband transitions and excites a carrier density of less than $10^{10}/\text{cm}^2$. The bandwidth of the laser is larger than the energy splitting between the bonding and antibonding exciton states of the coupled-well system.

The simulation results assuming all the longitudinal lifetimes $T_{11}=T_{22}=T_{33}=500$ ps and the dephasing times $T_{12}=T_{13}=T_{23}=2.75$ ps are shown in Fig. 8(b) in which the single-pulse response virtually disappears after 6 ps. Zero-phase two-pulse excitation will increase the magnitude of the signal and extend the duration of oscillations, which will eventually die out. The agreement between the theory and the experiment is very good. We have also calculated the time evolution of level populations for the zero-phase and the π-phase conditions, respectively. The results (not shown here) are almost the same as those in Figs. 5(a) and 5(b), respectively, since the

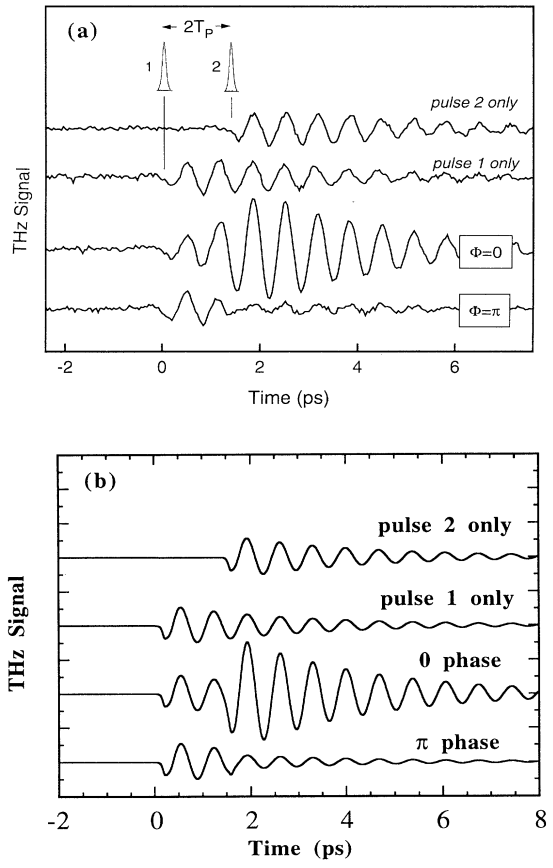

FIG. 8. (a) Experimental results for terahertz radiation from a coupled quantum well due to pulse 1 only, pulse 2 only, both pulses with a delay of $2T_p$, and a phase difference of 0 and π, respectively. The laser pumping is at the middle of level 1 and level 2 excitons. (After Ref. 11.) (b) Theoretical results for terahertz signals with finite relaxation times for the experimental conditions in (a). The exciton dephasing time is assumed to be 2.75 ps.

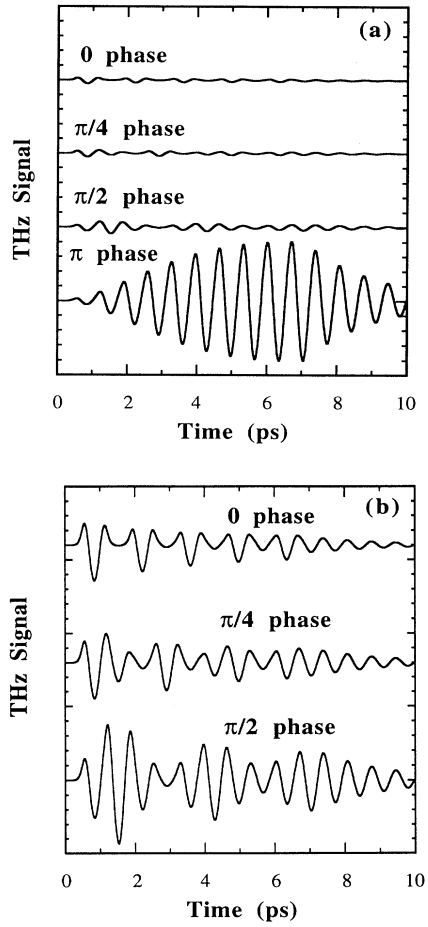

FIG. 9. (a) Calculated terahertz responses with a ten-pulse sequence. The relative phase between each pulse is chosen to be 0, $\pi/4$, $\pi/2$, and π, respectively. The separation time between two subsequent pulses is T_p. (b) A rescaled plot of (a) to show the features of 0, $\pi/4$, and $\pi/2$ phases.

decays of ρ_{11} and ρ_{22} are due to the longitudinal lifetime, which is very long (0.5 ns). The only change due to the finite dephasing time appears in $\rho_{12}(t)$, which, unlike the solid curve in Fig. 5(a), decays with a time constant of 2.75 ps as expected.

IV. MULTIPULSE-SEQUENCE EXCITATIONS

The control of charge oscillations by two-pulse excitation has been shown to be plausible. The next step would be to investigate the results of multipulse-sequence excitations. There are so many possible combinations that only one example will be shown. For a sequence of ten pulses with a fixed relative phase between each pair of nearby pulses, the results in Figs. 9(a) and 9(b) indicate a strong dependence on the relative phase. We see from Fig. 9(a) that the constructive interference for the π-phase case results in a signal which is at least ten times larger than the zero-phase signal. This result can also be compared with the two-pulse excitation results in Fig. 2 that the π-phase signal gives constructive interference and the zero-phase signal gives destructive interference for a time delay of only one charge-oscillation period. The zero-$\pi/2$ cases are enlarged in Fig. 9(b) to show the modulated features. It can be seen that the pulse shapes have fine structures depending on the phase difference and the time delay of the pulses. The charge-oscillation period is 689 fs; thus the duration of the ten-pulse sequence is about 7 ps. The ringing signals after 7 ps do not change as drastically except in magnitude. The response would change if a different set of relaxation time constants is used.

V. CONCLUSIONS

Both analytical results for terahertz radiation from coupled quantum wells due to coherent optical excitation assuming two δ pulses and numerical results for finite pulses have been shown. Our numerical results agree very well with the analytical results and the experimental data. We clearly show that the terahertz radiation field depends on the photon energy, the relative phase, and the pulse delay of the pumping optical pulses. Coherent control of quantum beats in a quantum-well system is demonstrated using two phase-locked optical pulses. These results will be very useful for the pulse shaping of a terahertz signal generated by optically pumping semiconductor quantum-well structures.

ACKNOWLEDGMENTS

We would like to thank K. Köhler for providing the sample. This work at the University of Illinois was supported by the Office of Naval Research under Grant No. N00014-90-J-1821. The computation time was provided by the National Center for Supercomputer Applications at the University of Illinois, Urbana-Champaign.

[1]H. G. Roskos, M. C. Nuss, J. Shah, K. Leo, D. A. B. Miller, A. M. Fox, S. Schmitt-Rink, and K. Köhler, Phys. Rev. Lett. **68**, 2216 (1992).

[2]K. Leo, J. Shah, E. O. Göbel, T. C. Damen, S. Schmitt-Rink, W. Schäfer, and K. Köhler, Phys. Rev. Lett. **66**, 201 (1991).

[3]X.-C. Zhang, B. B. Hu, J. T. Darrow, and D. H. Auston, Appl. Phys. Lett. **56**, 1011 (1990); X.-C. Zhang and D. H. Auston, J. Appl. Phys. **71**, 326 (1992).

[4]S. L. Chuang, S. Schmitt-Rink, B. I. Greene, P. N. Saeta, and A. F. J. Levi, Phys. Rev. Lett. **68**, 102 (1992).

[5]P. C. M. Planken, M. C. Nuss, W. H. Knox, and D. A. B. Miller, Appl. Phys. Lett. **61**, 2009 (1992).

[6]X.-C. Zhang, Y. Jin, K. Yang, and L. J. Schowalter, Phys. Rev. Lett. **69**, 2303 (1992).

[7]P. C. M. Planken, M. C. Nuss, I. Brener, K. W. Goossen, M. S. C. Luo, S. L. Chuang, and L. Pfeiffer, Phys. Rev. Lett. **69**, 3800 (1992).

[8]J. Agostinelli, G. Harvey, T. Stone, and C. Gabel, Appl. Opt. **18**, 2500 (1979).

[9]F. Spano, M. Haner, and W. S. Warren, Chem. Phys. Lett. **135**, 97 (1987); C. P. Lin, J. Bates, J. T. Mayer, and W. S. Warren, J. Chem. Phys. **86**, 3750 (1987).

[10]A. M. Weiner, J. P. Heritage, and E. M. Kirschner, J. Opt. Soc. Am. B **5**, 1563 (1988).

[11]P. C. M. Planken, I. Brener, M. C. Nuss, M. S. C. Luo, and S. L. Chuang, Phys. Rev. B **48**, 4903 (1993).

[12]Y. R. Shen, *The Principles of Nonlinear Optics* (Wiley, New York, 1984).

[13]S. L. Chuang, S. Schmitt-Rink, D. A. B. Miller, and D. S. Chemla, Phys. Rev. B **43**, 1500 (1991).

[14]L. Schultheis, A. Honold, J. Kuhl, K. Köhler, and C. W. Tu, Phys. Rev. B **43**, 9027 (1991).